INVESTIGATION OF THE SEMICONDUCTOR-METAL TRANSITION IN THE BISMUTH-ANTIMONY SYSTEM IN A MAGNETIC FIELD

N. B. BRANDT, E. A. SVISTOVA, and R. G. VALEEV

Moscow State University

Submitted March 20, 1968

Zh. Eksp. Teor. Fiz. 55, 469–485 (August, 1968)

The transition of a semiconductor to a metal in the presence of a magnetic field is studied in Bi-Sb alloys containing from 5 to 16 at. percent Sb. The investigation is carried out at a magnetic field strength of 450 kOe, at temperatures of 4 and 77°K, and for various orientations of the field and current relative to the crystallographic axes. It is shown that an energy gap appears in Bi-Sb alloys at antimony concentrations above 8 at. percent. The dependences of the gaps in the Bi-Sb spectra on the antimony concentration are obtained. It is shown that in semiconducting Bi-Sb alloys the critical fields for which the transverse electrical resistance drops sharply, and at which the alloys go over to the metallic state (with a temperature dependence of the resistance characteristic of metals) increase with increasing amount of antimony. Local minima which precede the transition to the metallic state have been detected on the resistance versus field strength curves. The minima are apparently due to changes in the energy spectra of the alloy in the magnetic field. The magnitude of the spin splitting of the Landau levels in Bi-Sb alloys is discussed.

INTRODUCTION

In[1] we reported the observation of a new phenomenon—the transition of a semiconductor to a metal in a magnetic field—which was observed in the system of semiconducting Bi-Sb alloys at a temperature of 4.2°K. This work is devoted to a detailed study of this phenomenon in Bi-Sb alloys in the 5 to 16 at. percent range of concentration of the second component in a magnetic field H up to 450 kOe and at temperatures of 4 and 77°K for various orientations of the field and current relative to the crystallographic axes of the samples[1)].

Metal-semiconductor and semiconductor-metal type transitions are connected with a displacement of the band boundaries and energy extrema in the bands in a magnetic field compared with their positions in the absence of a field. The possibility of such transitions and of the related singularities of the electric characteristics has been considered in[2] on the example of a quadratic dispersion law:

$$\varepsilon(p_x, p_y, p_z) = \frac{p_x^2}{2m_x} + \frac{p_y^2}{2m_y} + \frac{p_z^2}{2m_z} \quad \text{for } H = 0; \tag{1}$$

$$\varepsilon(n, p_z) = (n + 1/2)\frac{|e|\hbar}{m^* c}H \pm \frac{|e|\hbar}{2m^s c}H + \frac{p_z^2}{2m_z} \quad \text{for } H \neq 0$$

[m_x, m_y, m_z are the components of the effective-mass tensor, n is an integer, $m^* = (\pi/2)\partial S/\partial\epsilon$ and $m^s > 0$ are the cyclotron and spin effective masses of the current carriers].

The value of $\Delta\epsilon_i$ and the direction of the displacement of the i-th extremum is determined by the magnitude and sign of the parameter B_i:

$$B_i = \frac{1}{|m_i^*|} - \frac{1}{m_i^s}, \quad \Delta\varepsilon_i = \frac{|e|\hbar}{c}B_i H. \tag{2}$$

For $B_i < 0$ the energies of the minima are lowered and of the maxima raised; for $B_i > 0$—vice versa.

Since the main difference in the structure of the energy spectra of metals (with equal numbers of electrons n_e and holes n_h) and semiconductors consists in the fact that in the former the energy bands overlap, whereas in the latter there is an energy gap ΔE between the bands), then the displacement of the band boundaries in a magnetic field may lead to transitions of metals to the semiconducting state or of semiconductors to the metallic state. An essential condition for transitions of the former type is the requirement[2]

$$A = \frac{1}{|m_e^*|} - \frac{1}{m_e^s} + \frac{1}{|m_h^*|} - \frac{1}{m_h^s} > 0 \tag{3}$$

for the latter—$A < 0$ (the subscripts e and h denote electrons and holes).

Regardless of the exceptionally great complication of the general picture of the energy quantization in a magnetic field, for an arbitrary dispersion law the displacement of the band boundaries can in the first approximation be described by the following phenomenological relations.

For the bottom of the band (energy minima) we have

$$\Delta\varepsilon_e = \frac{e\hbar}{c}H\left|\frac{1}{m_e^*(p_z,\varepsilon)} - \frac{1}{m_e^s(p_z',\varepsilon)}\right|_{max} = \frac{e\hbar}{c}H|B_e^*|_{max},$$

if the bottom of the band is lowered, and

$$\Delta\varepsilon_e = \frac{e\hbar}{c}H|B_e^*|_{min},$$

if it is raised.

For the top of the band (energy maxima) we have

$$\Delta\varepsilon_h = \frac{e\hbar}{c}H\left|\frac{1}{m_h^*(p_z,\varepsilon)} - \frac{1}{m_h^s(p_z',\varepsilon)}\right|_{max} = \frac{e\hbar}{c}H|B_h^*|_{max}, \tag{4}$$

if the top is raised, and

[1)] C_1 is the bisector axis, C_2 is the binary axis, and C_3 is the trigonal axis.

$$\Delta\varepsilon_h = \frac{e\hbar}{c} H |B_h^*|_{min},$$

if it is lowered.

In these relations the effective masses $m^*(p_z, \epsilon)$ and $m^S(p_z', \epsilon)$ of the electrons at the bottom of the band and of holes at the top refer to such values of p_z and p_z' for which at an energy ϵ the modulus of B^* has an extremum.

If the relationship between the cyclotron and spin effective masses in expressions (4) is such that the band boundaries in a semiconductor draw closer in a magnetic field and move apart in the case of a metal, then for certain critical values of the magnetic field H_c there should occur semiconductor (dielectric at $T = 0^\circ K$) - metal and metal-semiconductor (dielectric at $T = 0^\circ K$) transitions respectively, independently of the dispersion law of the current carriers. Naturally, these effects will be most simple to observe in materials with a small band overlap or with a small energy gap ΔE. A very convenient object of investigation from this point of view is the Bi-Sb system.

On increasing the concentration of antimony which forms with bismuth a continuous series of solid solutions, the existing band overlap in bismuth decreases initially. According to data obtained in[3], in the 0 to 3 at. percent range of concentrations of antimony the overlap decreases linearly with the concentration from 38 meV in bismuth to 16 meV in the alloy $Bi_{97}Sb_3$. As far as we know, no data are available on the variation of the overlap at higher antimony concentrations. However, Jain[4] observed at 5 at. percent antimony the appearance of a gap which increased linearly in the range of concentrations from 5 to 12 at. percent antimony.

METHOD OF MEASUREMENT

The measurements were carried out on a setup for obtaining pulsed magnetic fields. The magnetic field was produced by a discharge of a bank of capacitors with a capacitance of 2000 μF charged to 2.7 kV by means of a coiled solenoid placed in a liquid-nitrogen bath. The construction of the solenoid was identical with that described by Karasik.[5] For an inner diameter of 8 mm and a 50-mm long operating portion of the solenoid the maximum field attained amounted to 500 kOe with a pulse duration of 3.6 μsec. The solenoid was connected to the capacitor bank by means of a gas discharger triggered by a 40-kV trigger pulse of ~1 μsec duration. The field strength was determined with the aid of a test coil directly connected to the plates of an oscillograph. For calibration a signal of known amplitude and period from a GZ-34 generator was supplied to these plates. The magnitude of the field was determined by integration of strongly magnified oscillograms.

The samples mounted in a special holder were placed in the narrow end of a helium dewar. The dewar with the holder were moved with the aid of a lifting device so that the sample was located at the center of the solenoid. The samples were cut from ingots prepared at the LGPI in the laboratory of G. I. Ivanov by electroerosion with a limitingly small rate of cut; the samples were in the form of right-angle parallelepipeds ~0.4 × 0.4 × 2.5 mm in dimension. The faces of the parallelepiped were parallel to the crystallographic axes of the crystal. After cutting, the surface layer was etched in a solution of nitric and hydrofluoric acid to a depth of no less than 50 microns.

The lower part of the sample holder consisted of a turned ivory cylinder of 2.5-mm diameter; the lower cross section of the cylinder was accurately perpendicular to its longitudinal axis. The sample was placed on this cross section and its ends were soldered over all their area with Wood's alloy to small strips of annealed 30-micron thick copper foil glued to the lateral sides of the cylinder and simultaneously serving as current electrodes. In order to insure that the measuring current remains constant during the measurements when the resistance of the sample increases strongly, a ballast resistance of about 5000 ohms was connected in series with the sample.

Potential electrodes of copper wire of 20 micron diameter were soldered to the samples by an electric spark method.[6] The maximum deviation of the soldering position from the longitudinal axis of the face of the sample did not exceed 20 μ. The distance between the electrodes varied between 0.6 and 1.2 mm.

The potential electrodes of 20-μ wire were soldered to thicker conductors located in the longitudinal groove of the cylinder holder and formed together with it a loop whose area was matched for maximum compensation of the induction during the field pulse. A small thin-walled organic-glass cup filled with diffusion oil, which froze on being cooled and fixed rigidly the current and potential electrodes, was then pulled over the end of the holder with the sample.

The voltage from the potential electrodes was supplied through a broad-band amplifier to the plates of a modernized OK-17 oscillograph. The oscillograph was triggered in synchronism with the magnetic-field pulse. In order to exclude completely induction pickup the oscillograms were obtained for two identical field pulses with opposite directions of the measuring current. The potential difference on the sample, proportional to its resistance, was determined as half the sum of the amplitudes of these oscillograms.

The depth of the skin layer of the measured samples exceeded by a large factor their transverse dimensions so that the effect of eddy currents could be neglected.

The possible increase in the temperature of the samples during the field pulse (thermal shock) due to the production of Joule heat did not exceed ~1°K for the largest measuring currents (20–30 mA). The temperature dependences of the electrical resistance of the samples in the absence of a magnetic field were measured by the block method, a gas thermometer being used to determine the temperature.

RESULTS OF THE MEASUREMENTS

1. Determination of the sample composition. It has been indicated above that the samples were cut from single-crystal ingots of the Bi-Sb alloy by electroerosion. To determine the sample composition, the parts of the ingots directly adjacent to the samples on the right and on the left along the direction of growth of the crystals were chemically analyzed. In order to exclude possible errors in carrying out the analysis, it

Table I

Sample No.	at. % Sb		$\frac{\rho(4.2°K)}{\rho(300°K)}$	ΔE, meV	direction of field*	H, kOe			
	calculation	analysis				H_1	H_2	$\tilde{H}$	H_K
1a	6.0	5.5	1,2	—	H ‖ C_3	—	—	—	—
1b	6.0	5.5	1,4	—	H ‖ C_1	—	—	—	—
2a	5.0	6,45	3,5	—	H ‖ C_3	—	—	—	—
2b	5.0	6.45	3,5	—	H ‖ C_1	—	—	—	—
3a	8.0	8.8	24	6.0	H ‖ C_3	—	—	—	20
3b	8.0	8,8	24	6.0	H ‖ C_1	—	—	—	—
4a**	9.0	8,9	45	13.0	H ‖ C_3	—	—	—	70
4b**	9.0	8.9	45	13.0	H ‖ C_1	—	—	—	—
5a***	7.0	9,1	215	15.6	H ‖ C_3	—	—	—	90
5b***	7.0	9.1	215	15.6	H ‖ C_1	—	—	—	—
6a**	10.0	10.5	300	13.5	H ‖ C_3	65	120	90	150
6b**	10,0	10.5	175	13.5	H ‖ C_3	65	120	90	150
6c**	10.0	10.5	212	13,5	H ‖ C_3	65	120	90	150
6d**	10,0	10.5	155	13.5	H ‖ C_3	—	—	—	150
7a****	9.0	—	122	17.4	H ‖ C_3	—	—	—	195
7b****	9.0	—	91	17.4	H ‖ C_3	—	—	—	195
7c****	9.0	—	50	17.4	H ‖ C_3	—	—	—	195
7d****	9.0	—	122	17.4	H ‖ C_1	—	—	—	—
7e****	9.0	—	91	17.4	H ‖ C_1	—	—	—	—
8a	12.0	12.0	236	15.7	H ‖ C_3	85	150	120	250
8b	12.0	11.5	19	14.4	H ‖ C_3	85	150	120	250
9a	15.0	15,8	26	19.0	H ‖ C_3	120	210	170	370
9b	15,0	15.8	26	19.0	H ‖ C_1	—	—	—	

*Direction of the measuring current i‖C_2.

**The chemical analysis for these samples was repeated.

***For these samples ρ_{max}/ρ (300°K) is cited.

****Samples from another batch.

was carried out twice. The results of the two analyses coincided within an accuracy of 0.1 wt. percent. The composition of the samples according to the data of the chemical analysis and the calculated antimony concentration in the alloys is given in Table I.

The appreciable discrepancy between the calculated data and the results of the chemical analysis indicates the presence of a considerable gradient in the antimony distribution along the length of the ingot. This circumstance apparently decreases the accuracy of the determination of the true antimony content in the samples from the data on the analysis of the adjoining portions of the ingot to several tenths of an at. percent.

2. The temperature dependences of the electrical resistance. In all the investigated samples the electritrical resistance increased on lowering the temperature from room temperature to ~20°K. On lowering the temperature further two types of temperature dependences were observed: a) a further increase of the resistance down to the lowest temperatures, b) an increase with a subsequent transition to saturation at liquid helium temperatures, and c) a decrease of the resistance, leading to the appearance of a maximum ρ_{max} on the $\rho(T)$ curves in the region of ~20°K.

It was noted that when the samples were damaged as a result of an abrupt change in the temperature or mechanical deformation, then the $\rho(T)$ dependences of type a) went over to dependences with the type b) saturation, and in type c) dependences the magnitude of the relative change of the resistance below 20°K decreased. At the same time, the ratio $\rho_{max}/\rho(300°K)$ —of the maximum value of the resistance at low temperatures to the resistance at 300°K—decreased in all the samples. The values of $\rho(4.2°K)/\rho(300°K)$ of the investigated samples are given in Table I. Characteristic types of $\rho(T)$ dependences are shown in Fig. 1.

Jain[4] interpreted the increase of the resistance on lowering the temperature in alloys containing more than 5 at. percent antimony as a result of the appearance of a gap ΔE in the energy spectrum of the alloys. In order to calculate the gap, we used the formula

$$\rho = \rho_0 e^{-\Delta E/2kT}, \quad (5)$$

which is valid for semiconductors having an intrinsic conductivity with the assumption that the mobilities of the current carriers vary as $T^{-3/2}$. One must, however, bear in mind that the increase of the resistance, with decreasing temperature can also be due to a small band overlap,[7,8] as a result of which the concentration of current carriers changes as $\sim T^{-3/2}$. In the latter case the T dependence of ρ should be a power law

$$\rho = \rho_0 T^m. \quad (6)$$

A careful analysis of the $\rho(T)$ dependences in Bi-Sb alloys in the range of concentrations 5 at. percent $< c <$ 16 at. percent antimony indicates that from 5 to 8 at. percent antimony they follow a power law (Fig. 2a) with an exponent $m \sim 1$ and only for $c >$ 8.5 at. percent do these dependences in the region of temperatures ~20–100°K become exponential (Fig. 2b). We note that in the samples investigated by Jain[4] the resistance increased on cooling only several-fold; the general form of the $\rho(T)$ dependences was rather complicated, so that it was in our view impossible to distinguish between the power and ex-

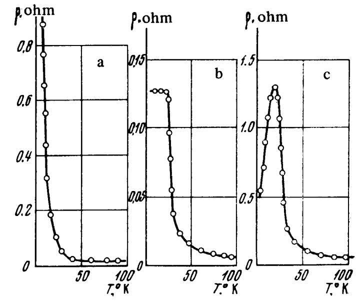

FIG. 1. Characteristic types of temperature dependences of the electrical resistance for semiconducting Bi-Sb alloys.

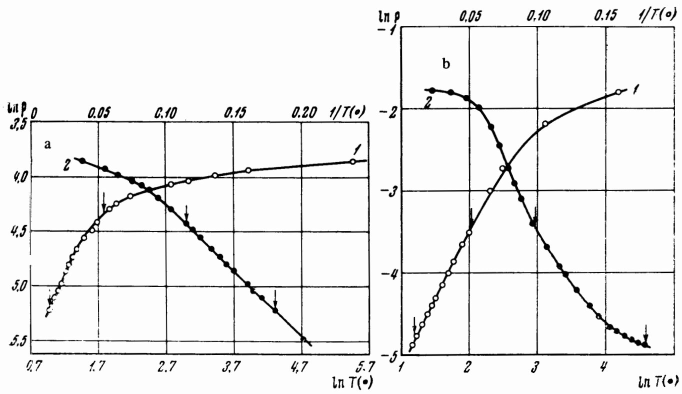

FIG. 2. Temperature dependence of the resistance for H = O for the samples: a—$Bi_{93.55}Sb_{6.45}$ and b—$Bi_{91.2}Sb_{8.8}$ in ln ρ–1/T coordinates (curve 1) and ln ρ–ln T coordinates (curve 2). The temperature is in °K. The arrows mark the range from 20 to 100°K.

ponential dependence in alloys containing from 5 to 8--9 at. percent antimony.

The gaps ΔE calculated according to (5) for the Bi-Sb samples investigated by us ($c > 8.5$ at. percent Sb) are given in Table I. It is interesting to note that for samples of the same composition but of different quality [different ratio $\rho_{max}/\rho(300°K)$] the gaps ΔE have within the accuracy of the measurements the same value, regardless of the fact that the $\rho(T)$ dependences of these samples below 15–20°K differ appreciably.

3. Dependence of the resistance on the magnetic field. At an antimony concentration below 8 at. percent the electrical resistance increases monotonically in a magnetic field for all orientations of the field relative to the crystallographic axes of the samples (Fig. 3). A characteristic feature of these dependences is a strong decrease of the anisotropy of the magnetic resistance in strong fields, connected with the different character of the $\rho(H)$ dependences at field orientations parallel and perpendicular to the trigonal C_3 axis. In weak fields (below ~100 kOe) ρ increases more rapidly for $H \parallel C_3$ than for $H \perp C_3$. In the range of strong fields for $H \parallel C_3$ the $\rho(H)$ dependence reveals a tendency towards saturation, whereas for $H \perp C_3$ in the range of fields above 100–150 kOe it is close to linear. As a result of this the anisotropy of the alloy $Bi_{93.1}Sb_{6.9}$ decreases in a field $H \approx 400$ kOe to less than a half.

In alloys containing more than 8.5 at. percent antimony the character of the $\rho(H)$ dependences changes qualitatively: for a field orientation parallel to the trigonal axis a sharp decrease is observed with increasing field in all the investigated samples for some value of the field H_c depending on the composition of the alloy. The value of H_c increases monotonically on increasing the antimony concentration in the alloys. For field orientations perpendicular to the trigonal axis this effect is absent.

Regardless of the fact that the decrease of the resistance for $H > H_c$ is the most characteristic feature of the behavior of alloys containing more than 8.5 at. percent antimony, a number of peculiarities are observed in the $\rho(H)$ dependences which make it possible to separate two subranges of antimony concentrations (at. percent): $8.5 < c < 9.5$ and $c > 9.5$.

In the first subrange, on increasing the field directed parallel to the trigonal axis the resistance first increases, goes through a maximum at $H = H_c$, and then decreases, approaching some constant value which in the region of strong fields depends weakly on the field strength (Fig. 4). In a field perpendicular to the trigonal axis the resistance increases in weak fields faster than H, then for H ~ 50--100 kOe it bends and continues to increase monotonically approximately proportionally to H. On increasing the gap ΔE the anisotropy of the magnetic resistance in weak fields ($H < H_c$) decreases rapidly. In a field H = 20 kOe in an alloy with ΔE = 6 meV the value of $\rho(H \parallel C_3)/\rho(H \perp C_3) \approx 6$, in an alloy with ΔE = 13 meV it is ≈3, and in an alloy with ΔE = 15.6 meV it

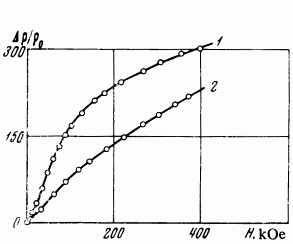

FIG. 3. Dependence of the resistance on the magnetic field for the $Bi_{93.55}Sb_{6.45}$ sample. Curve 1—$H \parallel C_3$, $i \parallel C_2$; curve 2—$H \parallel C_1$, $i \parallel C_2$, T = 4.2°K.

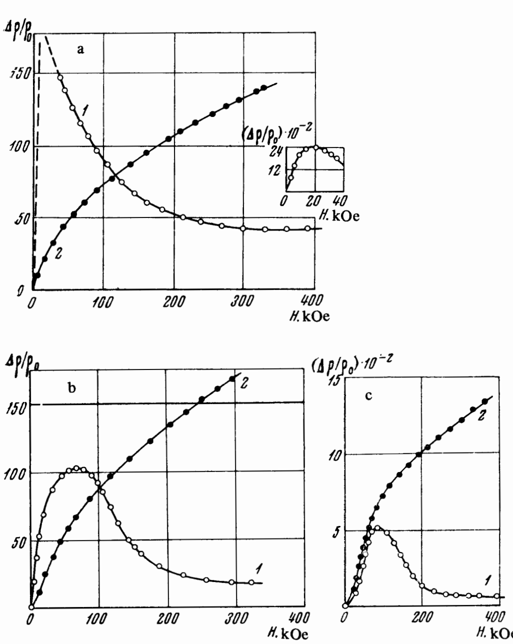

FIG. 4. Dependence of the resistance on the magnetic field for samples of the following composition: a—$Bi_{91.2}Sb_{8.8}$, b—$Bi_{91.1}Sb_{8.9}$, c—$Bi_{90.9}Sb_{9.1}$. Curve 1—$H \parallel C_3$, $i \parallel C_2$; curve 2—$H \parallel C_2$, $i \parallel C_2$, T = 4.2°K.

amounts to ≈1 (Fig. 4). As a result in the first two alloys on going through H_c the anisotropy changes sign, whereas in the third alloy it only increases sharply.

In the second subrange ($c > 9.5$ at. percent antimony) a local resistance minimum appears in the region of the maximum on the $\rho(H)$ dependence for $H \parallel C_3$ (Figs. 5 and 6); the depth of this minimum increases with increasing antimony concentration and its position shifts towards the region of higher fields. The depth of the local minimum depends strongly on the quality of the sample [the value of $\rho_{max}/\rho(300°K)$]. On damaging the same sample the position of the local minimum does not change, whereas its depth decreases gradually; as a result of this the minimum ceases to be noticeable (Fig. 5). In samples with a large $\rho_{max}/\rho(300°K)$ ratio the resistance decreases for $H > H_c$ by a factor of several hundred and attains a value which is in any case smaller than the resistance at $H = 0$ (Fig. 6, curve b). In these instances one can only state that the absolute value of the resistance becomes less than the measurement accuracy of 0.2 ohm.

In the best samples the effect of the decrease of the resistance in a field is also observed at the liquid nitrogen temperature of 77°K (Fig. 7). However, the increase of the resistance with the field at this temperature is considerably smaller than at 4.2°K, the maximum is smeared out, the local minimum disappears, the resistance begins to decrease at large values of the magnetic field and decreases only by 30–40 percent. In less perfect samples the resistance at liquid nitrogen temperatures increases monotonically with the field, exhibiting no decreasing trend.

DISCUSSION OF THE RESULTS

1. A criterion for the quality of Bi-Sb single crystals. It was shown in[9] that the presence of defects in the lattice, in particular those related to the nonuniform distribution and incomplete solution of the second component, as well as those related with a small plastic deformation, leads to a smearing of the extrema of the bands and the production of "tails" with a low density of states. The depth of the smearing and the density of states in it depend on the number of defects and impurity atoms in the lattice and the degree of its perfection.

The presence of "tails" in the valence and conduction bands leads to the circumstance that a residual conductivity connected with the band overlap remains in the semiconducting region, even in the case of alloys prepared from extremely pure components. Therefore, the more perfect the crystals, the smaller the residual conductivity at $T \to 0°K$. From this point of view the absence of saturation of the resistance on the $\rho(T)$ curves down to the very lowest temperatures and the value of the ratio $\rho(T \to 0°K)/\rho(300°K)$ are the most reliable criteria for the perfection of crystals.

The increasing energy length of the "tails" and of the density of states within them, accompanied by decrease of the ratio $\rho(T \to 0°K)/\rho(300°K)$, explains naturally the smearing out of the features on the $\rho(H)$ curves when the samples are damaged. Damaging the samples which leads to increasing concentration of current carriers is to some extent equivalent to a temperature increase.

Retention of the residual conductivity at low temperatures can also be connected with an unequal concentration of electrons and holes resulting from the presence of acceptor-donor type impurities in the alloys. In this case, even if the band structure is perfect, the electrical conductivity of the alloys will be determined after freezing out the excited current carriers by the magnitude of the excess concentration of electrons or holes.

For a sufficient degree of "contamination" and

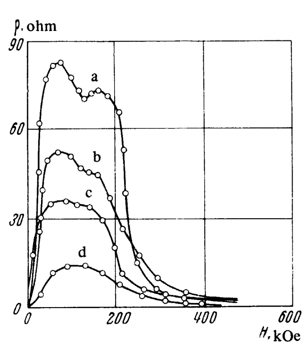

FIG. 5. $\rho(H)$ dependence for $Bi_{89.5}Sb_{10.5}$ samples with various ratios of $\rho(4.2°K)/\rho(300°K)$ for $H \parallel C_3$, $i \parallel C_2$; $T = 4.2°K$: a–$\rho(4.2°K)/\rho(300°K) = 300$, b–212, c–175, d–135.

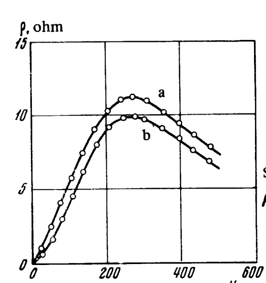

FIG. 7. $\rho(H)$ dependence for $Bi_{89.5}Sb_{10.5}$ samples for $H \parallel C_3$, $i \parallel C_2$, $T = 78°K$. Curve a–$\rho(4.2°K)/\rho(300°K) = 300$, b–212.

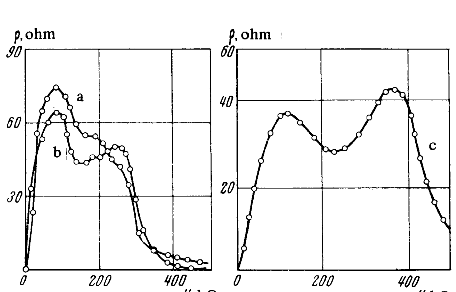

FIG. 6. $\rho(H)$ dependence for the following samples: a–$Bi_{88.5}Sb_{11.5}$, b–$Bi_{88}Sb_{12}$, and $Bi_{84.2}Sb_{15.8}$ for $H \parallel C_3$, $i \parallel C_2$, $T = 4.2°K$.

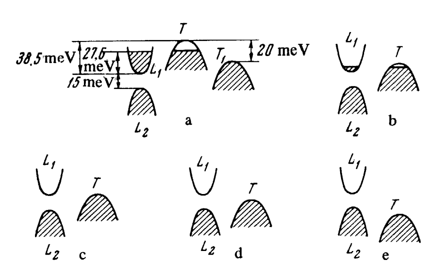

FIG. 8. Change of the energy spectrum of bismuth on adding antimony: a–energy spectrum of pure bismuth, b–e–successive change of the energy spectrum of bismuth with increasing antimony admixture.

perfection of the lattice a maximum should appear on the temperature curves $\rho(T)$; this was observed, for example, in the alloy $Bi_{90.9}Sb_{9.1}$ (Fig. 1). In such "impurity" samples the ratio of resistances at the maximum and at T = 300°T, i.e., $\rho_{max}/\rho(300°K)$, can serve as a criterion of the quality of the lattice, and the ratio $\rho(T \to 0°K)/\rho(300°K)$ as an indirect criterion of the contamination. The smaller the latter ratio, the more strongly "contaminated" the sample. The high values of $\rho(4.2°K)/\rho(300°K)$ in the majority of the investigated samples attest to their high degree of perfection.

2. The change of the energy spectrum in Bi-Sb alloys. According to existing ideas,[10-14] the energy spectrum in Bi-Sb alloys changes as follows (Fig. 8).

On increasing the antimony concentration the extrema of the valence bands T and T′ in the bismuth spectrum are lowered relative to the extrema L_1 and L_2, the distance E_g between which remains unchanged

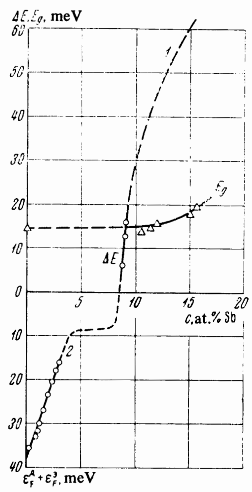

FIG. 9. Variation of the magnitude of the overlap in the "metallic" Bi-Sb alloys (with less than 8.5 at. percent Sb) and of the gaps E_g (between the extrema L_1 and L_2) and ΔE (L_1 and T).

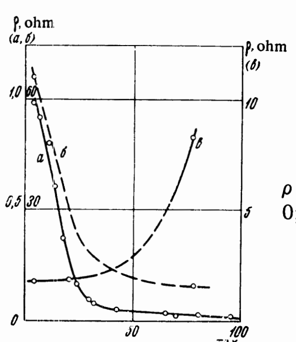

FIG. 10. Temperature dependence of ρ for the $Bi_{89.5}Sb_{10.5}$ sample for: a—H = 0; b—H<H_c; c—H>H_c.

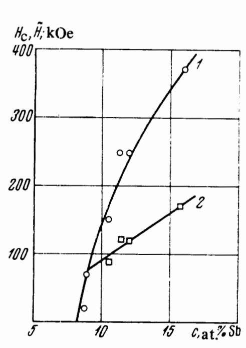

FIG. 11. Dependence of the critical field H_c (curve 1) and of the field $\tilde{H}$ (curve 2) on the antimony concentration.

in a first approximation. In the range of concentrations $0 < c < 3.0$ at. percent antimony the band overlap decreases approximately in proportion to the antimony concentration[15] (Fig. 9). On the basis of a linear extrapolation of this dependence one would expect that for c = 5 at. percent antimony the band overlap vanishes, which is in agreement with the results of Jain.[4] However, as was indicated above, in the range of concentrations from 5 to 8.5 at. percent antimony the band overlap is retained and the energy gap only appears at antimony concentrations exceeding 8.5 at. percent (Fig. 8d).

The values of the gaps calculated from the $\rho(T)$ curves for the investigated samples are shown in Fig. 9. The gap width increases rapidly in the range of concentrations from 8.5 to 9.5 at. percent antimony, after which it changes weakly. Such a character of the change of the gap means that the extremum T being lowered together with T′ becomes at c = 9.5 at. percent antimony equal to the extremum of light holes L_2 (Fig. 8). On being lowered further, the gap between the extrema L_1 and T becomes larger than the gap E_g (Fig. 8e). Therefore the experimental data obtained for $c > 9.5$ at. percent antimony refer to the gap E_g and characterize its dependence on the concentration. The values of the gap E_g obtained in this range of concentrations are in good agreement with the value of E_g = 15 meV in bismuth.[15,16] The gap E_g apparently does not change for concentrations $0 < c < 12$ at. percent antimony and then increases weakly. The proposed nature of the change of the gap ΔE between the extrema L_1 and T at concentrations $c > 9.5$ at. percent antimony based on the results of measurements of the magnetic resistance (see below) is shown in Fig. 9 by the dashed line 1.

In order to reconcile the data on the change of the band overlap in alloys with an admixture of up to 3.0 at. percent antimony with the obtained dependence of the gap ΔE on the antimony concentration, one must assume that in the range of 3.0 at. percent Sb $< c <$ 8.5 at. percent Sb the band overlap in Bi-Sb alloys changes in irregular fashion. It is quite possible that the irregular nature of the dependence of the overlap on the antimony concentration in the range preceding the appearance of the gap is a manifestation of the "delay" effect of the metal-semiconductor transition connected with the fact that the transition is energetically disadvantageous. Since in bismuth a state with a small band overlap is more advantageous than the "dielectric" state,[17] then on increasing the antimony concentration above 3 at. percent the crystal lattice of the alloys can be deformed in such a way that the overlap is retained until the energy of the lattice deformation compensates for the energy gained at the expense of the band overlap. As soon as the deformation energy becomes equal to the overlap energy, the latter decreases sharply (jumpwise in the ideal case) and an energy gap appears in the spectrum of the alloys.

An analogous effect can take place in the transition of Bi-Sb alloys from the "metallic" to the semiconducting state under pressure. The work of Itskevich and Fisher[18] in which they investigated quantum oscillations connected with the hole surface in a Bi-Sb alloy under a pressure of 10 kbar is of interest from this point of view. They observed that the extremal cross section of the hole surface of this alloy decreases weakly under compression in the range of pressures ~7 kbar, and decreases subsequently very rapidly to zero. Since hydrostatic compression and the antimony impurity give rise to analogous changes in the band overlap in bismuth, one can assume on the basis of the data of Itskevich and Fisher that the delayed change in the overlap begins at an antimony concentration above 3 at. percent. The possible form of the concentration dependence of the overlap is shown in Fig. 9 by the dashed curve 2.

We note that the elastic deformation energy W of the lattice under hydrostatic compression $W = P^2/2U$ (U is the volume compressibility) amounts at P ~ 7 kbar to ~6 meV which agrees in order of magnitude with the energy gain ($\sim E_F$ for holes) due to the overlap retained in the range of concentrations 4–8 at. percent antimony.

3. Semiconductor-metal transition in a magnetic field. It was noted above that the most characteristic peculiarity of the $\rho(H)$ dependence of Bi-Sb alloys containing more than 8.5 at. percent antimony when the field is directed parallel to the trigonal axis is the sharp decrease of the resistance when the field reaches the critical values H_c. A direct proof of the fact that this effect is a result of the appearance at $H = H_c$ of band overlap is the appearance for $H > H_c$ of a temperature dependence of ρ characteristic of metals (Fig. 10). The $\rho(T)$ dependence for H = 0 (curve a) and for $H < H_c$ (curve b) typical for semiconductors goes over to a metallic dependence (curve c) in fields exceeding H_c. The values of H_c for the investigated alloys are shown in Fig. 11.

The minimum concentration of antimony in alloys (~8.8 at. percent) starting with which there appears the effect of the resistance decrease in a field correlates well with the concentration at which a gap appears in the energy spectrum of the alloys (Fig. 9). A correlation is also observed between the $H_c(c)$ dependences in the range of concentrations 8.5 at. percent Sb < c < 9.5 at. percent Sb (Figs. 9 and 11) and the magnitude of the gap $\Delta E(c)$ in the corresponding concentration range.

The large negative value of the coefficient B [formula (2)] for holes at the extremum T in bismuth when the field is directed parallel to the trigonal axis ($m_h^s/m_h^* \approx 2$) retained in Bi-Sb alloys in the range of concentrations[2)] 0–4 at. percent antimony, the absence of the effect of decreasing ρ with increasing H for other orientations of the latter for which B > 0 for holes at the extremum T, as well as the correlation of the $H_c(c)$ dependences and $\Delta E(c)$ noted above for 8.5 at. percent Sb < c < 9.5 at. percent Sb indicate that a decrease of the gap in semiconducting Bi-Sb alloys in a magnetic field parallel to the trigonal axis, leading to the appearance of overlap for $H = H_c$, is mainly connected with a raising of the extremum T in the magnetic field.

It is therefore of interest to attempt to utilize the $H_c(c)$ dependence (Fig. 11) to determine the gap ΔE between the extrema T and L_1 in the range of concentrations exceeding 9.5 at. percent antimony where the direct determination of $\Delta E(c)$ from the $\rho(T)$ curves for H = 0 becomes impossible. Since there are no grounds for assuming that the value of the coefficient B for holes at the extremum T in bismuth increases (in magnitude) in Bi-Sb alloys, the bending of the H_c curve towards saturation (Fig. 11) means that the rate of displacement of the extremum T relative to L_1 in the alloys decreases with increasing antimony concentration. Unfortunately, it is impossible to determine to any accurate extent the dependences $\Delta E(c)$ solely on the basis of data obtained in this work. The dashed curve 1 shown in Fig. 9 is plotted with allowance for a number of approximate simplifications discussed below and is an estimate. We note that the decisive influence of the orientation on the nature of the $\rho(H)$ dependences excludes the possibility of explaining the observed anomalies on the basis of a change in the kinetics of the electrons in a magnetic field.

4. The local minimum on the $\rho(H)$ curve. We noted above that no local minimum is observed on the $\rho(H)$ curves in the concentration range 8.5 at. percent Sb < c < 9.5 at. percent Sb, and it appears only at high concentrations. Two reasons can apparently be cited which can lead to the appearance of a local minimum on the $\rho(H)$ curves: the presence of a large excess concentration of holes in the alloys as a result of the presence in them of acceptor-type impurities (for example, lead), and the interaction of the extrema L_1 and L_2 located one below the other when they draw closer together in a magnetic field.

In the first case one can propose the following scheme explaining the observed complex nature of the $\rho(H)$ dependences in the region preceding the transition of the semiconductor to the metal (Figs. 5 and 6). In alloys with a concentration larger than 9.5 at. percent antimony in zero field the excess holes occupy three L_2 extrema (Fig. 12a). On increasing the field the extremum T rises and reaches for some field H_1 the Fermi level of holes at L_2 (Fig. 12b). On further increasing the field the holes flow over from the L_2 extrema to the extremum T (Fig. 12c), as a result of which the hole extremum T is included in the electrical conductivity and the resistance decreases. For $H = H_2$ all the holes from the extremum L_2 "flow over" into the extremum T. Light holes belonging to L_2 are excluded from the electrical conductivity and the resistance again begins to increase. After the

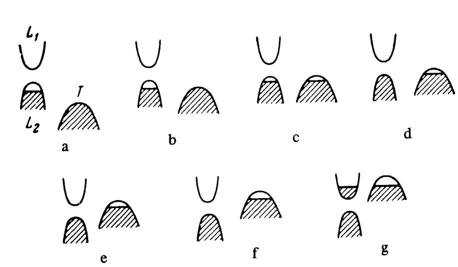

FIG. 12. Schematic diagram of the displacement of the extrema in Bi-Sb alloys in a magnetic field with $H \parallel C_3$. The field increases from a to g.

[2)]Results of an investigation of Bi-Sb alloys in the range of concentrations from 0 to 5 at. percent antimony in fields up to 500 kOe will be published in the nearest future.

Table II

	H ∥ C_1		H ∥ C_2		H ∥ C_3	
	m^*	m^s	m^*	m^s	m^*	m^s
Electrons	0.0084	0.0079	0.128	0.36	0.065	0.11
	0.0168	0.0158	0.0097	0.0091		
Holes	0.21	1.5	0.21	1.5	0.064	0.033

Fermi level reaches for $H = H_c$ the bottom of the conduction band (L_1), band overlap appears and the electrical conductivity increases sharply. The proposed scheme explains the absence of a local minimum in the range of concentrations between 8.5 and 9.5 at. percent antimony in which the extremum T is located above L_2 ($\Delta E < E_g$) and the increase of the local minimum on increasing the antimony content in the alloys as a result of an increase of the energy intervals $\Delta E - E_g$ and E_g.

It is natural to assume that a field $\tilde{H} = (H_1 + H_2)/2$ corresponds to the situation depicted in Fig. 12c. The values of the fields $\tilde{H}$ for the investigated samples are given in Fig. 11 (curve 2). Our attention is drawn to the fact that curve 2 intersects curve 1 at a point corresponding to the concentration c = 9.5 at. percent (for c > 9.5 at. percent the local minimum cannot appear). This value of the concentration is in good agreement with the value at which ΔE becomes equal to E_g (Fig. 9) (for $\Delta E \le E_g$ the local minimum obviously also cannot appear).

In the second case the drawing together of the extrema L_1 and L_2 in a magnetic field (on account of the rising of the extremum L_2) which precedes the overlap of the extrema L_1 and T (the semiconductor-metal transition) can also lead to an increase in the electrical conductivity and the appearance of a minimum on the $\rho(H)$ curve. We note that the extrema L_1 and L_2 cannot intersect in a magnetic field, a circumstance which would lead to band overlap.

The drawing together of the extrema L_1 and L_2 also makes it possible to explain the absence of local minima on the $\rho(H)$ curves in the range of concentrations below 9.5 at. percent antimony. Further investigations are essential in order to explain the real reason for the appearance of a local minimum.

5. Some remarks concerning the orbital and spin effective masses and their relations in the Bi-Sb alloys. In considering this question we shall assume that the general picture of the relations of spin and orbital effective masses in Bi-Sb alloys is qualitatively similar to that in bismuth. According to the data of[16], the effective masses in bismuth for a field orientation parallel to the principal crystallographic axes have the values shown in Table II. The cited values correspond to a quadratic dispersion law for holes and an ellipsoidal model with the nonquadratic Lax-cohen dispersion law[19,20] for the electrons.

The strong dependence of the cyclotron mass of the electrons on the energy is connected with the smallness of the gap E_g. In the case of holes in bismuth the corresponding gap E_g^T is in any event not smaller than 50–60 MeV.[17] Therefore in bismuth the deviation of the dispersion law from a quadratic one is not large in the case of holes, and can only lead to a certain de-

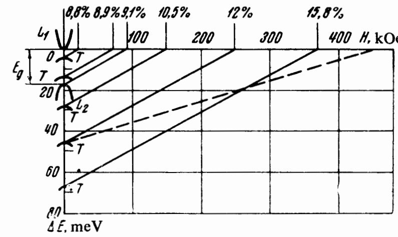

FIG. 13. Schematic diagram of the possible displacement of the extrema T (continuous lines) in Bi-Sb alloys in a magnetic field parallel to the trigonal axis. The dashed line characterizes the rate of displacement of T in bismuth. [16]

crease (by 30–40 percent) of the values of the cyclotron masses at the top of the band. Apparently, the energy dependence of the cyclotron masses of the holes should decrease in Bi-Sb alloys as a result of an increase of E_g^T.

It must immediately be emphasized that on the sole basis of the obtained experimental data it is impossible to obtain unique quantitative data on the values of m_e^*, m_h^*, m_e^s, and m_h^s and their relations in Bi-Sb alloys. First, there are no data on the nature of the change of the effective masses on increasing the antimony concentration. Secondly, we do not know how the values of the effective masses change when the spectrum changes in a magnetic field. Thirdly, it is not clear whether the relation of the spin and orbital masses remains the same in a strong magnetic field.

We restrict ourselves therefore only to a consideration of the problem to what extent the assumptions concerning the constancy of the masses of holes (constant rate of displacement of the hole extremum in a magnetic field) agrees with the obtained experimental data. This assumption is certainly incorrect for elec-) trons and holes at the extrema L_1 and L_2, since the values of the masses at the bottom of the band at L_1 and at the top at L_2 are determined by the magnitude of the gap E_g which can change strongly in a field.

Let us describe the displacement picture of the extrema T in a magnetic field (Fig. 13) assuming the displacement rate to be constant (linear approximation). On the ordinate axis we mark the proposed position of the extrema L_1 and L_2 in the investigated alloys for H = 0. On increasing the field the extrema L and T are displaced. We mark on the abscissa axis values of $H_c(c)$ and draw vertical straight lines through these points. The appearance of overlap for $H = H_c$ means that the lines describing the displacement of the extrema L_1 and T(c) in a magnetic field should intersect with the corresponding vertical straight line at one point.

Let us first consider the results obtained when the field is directed parallel to the bisector axis; these characterize the displacement of the extremum L_1. For this orientation the extremum T is lowered very slowly since the spin mass exceeds considerably the orbital mass and the latter is rather large. According to[16] the extremum L_1 should also be lowered at a rate $\partial E/\partial H = 0.1$ meV/kOe (dashed line on Fig. 14). It is seen that in the alloy $Bi_{91.2}$-$Sb_{8.8}$ with a value of $\Delta E = 6$ meV both straight lines intersect at

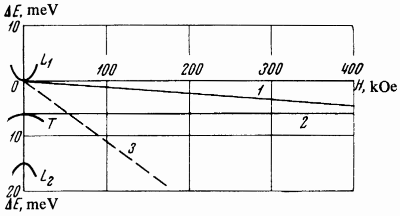

FIG. 14. Schematic diagram of the possible displacement of the extrema L_1 (line 1) and T (line 2) of Bi-Sb alloys in a field $H \parallel C_1$. The straight line 3 characterizes the displacement of L_1 in bismuth. [16]

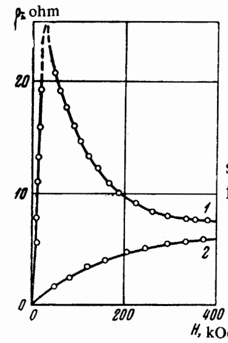

FIG. 15. $\rho(H)$ dependence for the following samples: 1 – $Bi_{91.2}Sb_{8.8}$ and 2 – $Bi_{93.55}Sb_{6.45}$ for $H \parallel C_3$, $i \parallel C_2$, T = 4.2°K.

H = 55 kOe, i.e., for this field band overlap should have appeared.

However, nothing of the sort is observed experimentally: even in the alloy with a gap width ΔE = 6 meV the resistance increases monotonically in the entire range of fields (Fig. 4, curves 2). Therefore, if there occurs overlap for this orientation, then for values of $H_c > 450$ kOe. It follows hence that L_1 is displaced downwards very weakly or is altogether not displaced, i.e., the corresponding value $|B| < 4$ (according to[16] $|B| = 32$). We note that for $H \parallel C_1$ the rate of displacement of L_1 downwards should have a maximum. For other orientations L_1 can altogether not descend or descends very slowly.

Let us now return to a consideration of the picture of the motion of the extrema in a field for $H \parallel C_3$ when overlap occurs. For simplicity we shall assume that the position of L_1 does not change in a field. We draw through the points H_c on the abscissa axis straight lines with a slope $e\hbar|B|/c$, the same as for the $Bi_{91.2}Sb_{8.8}$ sample for which both H_c and the gap between L_1 and T are known. Unfortunately, the use of the 8.5—9.5 at. percent antimony range for determining the value of $\partial\epsilon/\partial H$ is not correct, since in this range there may be appreciable effects connected with nonequilibrium processes when the lattice parameters change on account of a transition of the alloys from the metallic to the semiconducting state. The points of intersection of these straight lines with the ordinate axis should yield the values of the gaps ΔE in the investigated alloys. The values of ΔE thus obtained are shown in Fig. 9 by the dashed curve 1. The dashed curve on Fig. 13 characterizes the rate of displacement of the extremum T in bismuth in accordance with the data of[16].

6. The nature of the $\rho(H)$ dependence in Bi-Sb alloys for a concentration $c < 8.5$ at. percent Sb and $c > 8.5$ at. percent Sb. In alloys with $c < 8.5$ at. percent antimony the bands overlap for H = 0 and this overlap increases in a magnetic field. For $c > 8.5$ at. percent antimony the bands do not overlap for H = 0 and their overlap appears only in a magnetic field $H = H_c$. It would therefore appear that the nature of the $\rho(H)$ dependences after the appearance of overlap in alloys with $c < 8.5$ and $c > 8.5$ at. percent antimony should be identical. Figure 15 shows $\rho(H)$ curves for two Bi-Sb alloys located on the left and on the right of the concentration c = 8.5 at. percent antimony. It is seen that in the range of strong fields the absolute values of the electrical conductivities and the form of the $\rho(H)$ curves in these alloys are similar. The strong increase of the resistance for $H < H_c$ of the $Bi_{91.2}Sb_{8.8}$ alloy characterizes its semiconducting behavior in a magnetic field.

In conclusion we express our deep gratitude to Professor G. I. Ivanov for kindly providing single-crystal Bi-Sb samples of very high quality, M. Ya. Azbel' for useful discussions and interest in the work, as well as to Yu. G. Kashirskiĭ and V. Lyn'ko for assistance in carrying out the experiments.

[1] N. B. Brandt, E. A. Svistova, and R. G. Valeev, ZhETF Pis. Red. 6, 724 (1967) [JETP Lett. 6, 203 (1967)].
[2] M. Ya. Azbel' and N. B. Brandt, Zh. Eksp. Teor. Fiz. 48, 1206 (1965) [Sov. Phys.-JETP 21, 804 (1965)].
[3] N. B. Brandt, L. G. Lyubutina, and N. A. Kryukova, Zh. Eksp. Teor. Fiz. 53, 134 (1965) [Sov. Phys.-JETP 26, 93 (1968)].
[4] A. L. Jain, Phys. Rev. 114, 1518 (1959).
[5] V. R. Karasik, Prib. Tekh. Éksp. No. 1, 142 (1959).
[6] N. B. Brandt, Prib. Tekh. Éksp. No. 2, 138 (1956).
[7] I. M. Lifshitz and M. I. Kaganov, Usp. Fiz. Nauk 59, 419 (1959) and 78, 441 (1962) [Sov. Phys.-Uspekhi 5, 878 (1963)].
[8] D. Balla and N. B. Brandt, Zh. Eksp. Teor. Fiz. 47, 1653 (1964) [Sov. Phys.-JETP 20, 1111 (1965)].
[9] N. B. Brandt and Ya. G. Ponomarev, Zh. Eksp. Teor. Fiz. 55, No. 10 (1968) [Sov. Phys.-JETP, in press].
[10] N. B. Brandt and V. V. Shchekochikhina, Zh. Eksp. Teor. Fiz. 41, 1412 (1961) [Sov. Phys.-JETP 14, 1008 (1962)].
[11] S. Tanuma, J. Phys. Soc. Japan 14, 1246 (1959).
[12] S. Tanuma, J. Phys. Soc. Japan 16, 2349 (1961) and 18, 2354 (1963).
[13] G. A. Ivanov, Fiz. Tverd. Tela 5, 2409 (1963) [Sov. Phys.-Solid State 5, 1754 (1964)].
[14] N. B. Brandt and Ya. G. Ponomarev, Zh. Eksp. Teor. Fiz. 50, 367 (1966) [Sov. Phys.-JETP 23, 244 (1966)].
[15] N. B. Brandt and L. G. Lyubutina, Zh. Eksp. Teor. Fiz. 52, 686 (1967) [Sov. Phys.-JETP 25, 450 (1960)].
[16] G. E. Smith, G. A. Baraff, and J. M. Rowel, Phys. Rev. 135, A1118 (1964).
[17] A. A. Abrikosov and L. A. Fal'kovskiĭ, Zh. Eksp.

Teor. Fiz. **43**, 1083 (1962) [Sov. Phys.-JETP **16**, 765 (1963)].
[18] E. S. Itskevich and L. M. Fisher, ZhETF Pis. Red. **6**, 748 (1967) [JETP Lett. **6**, 219 (1967)].
[19] B. Lax, J. G. Havzoides, H. J. Zeiger, and R. J. Keyes, Phys. Rev. Letters **5**, 241 (1960).
[20] M. H. Cohen, Phys. Rev. **121**, 387 (1961).

Translated by Z. Barnea
55